

The exciton size: Where are the limits?

O.P. Dimitriev

V. Lashkaryov Institute of Semiconductor Physics, National Academy of Sciences of Ukraine,
41, prosp. Nauky, 03680 Kyiv, Ukraine
E-mail: dimitr@isp.kiev.ua

Abstract. The concept of exciton implies a collective excited state able to travel in a particle-like fashion. Its size is determined by the radius of excited electron-hole pair and, although it may vary by two orders of magnitude, it is always spatially restricted, while its delocalization length owing to the exciton wavefunction spatial dynamics may provide even a larger scale of changes. In this work, the limitations of exciton sizes are discussed by analysis where the exciton concept is still applicable. It is shown that the exciton size can be as small as few angstroms, but even smaller sizes can be, probably, justified. At the same time, coupling of exciton to polariton mode can enlarge the exciton-polariton coherence length to values as high as 20 μm , thus extending the scale of possible exciton sizes up to five orders of magnitude.

Keywords: Wannier–Mott exciton, Frenkel exciton, delocalization, self-trapping, low-dimensional media, Rashba effect.

<https://doi.org/10.15407/spqeo25.04.372>

PACS 71.35.-y

Manuscript received 18.08.22; revised version received 03.10.22; accepted for publication 14.12.22; published online 22.12.22.

1. Introduction

A simplified model of exciton is often presented as an excited electron-hole pair bound by the Coulomb attraction. However, in the early works the exciton was treated as collective excitation of atoms in a crystalline lattice [1]; therefore, the above definition is not full, because it does not take into account collective nature of the exciton that imposes specific features and which differentiates the exciton from a single-electron excitation of an isolated atom or a molecule. The collective nature of exciton can be considered using two ways. The two aspects of collective optical excitations are related to strong and weak coupling regimes, respectively, between excited subunits of the system. First, strong coupling, when all subunits of the system are excited coherently, in terms of the models proposed by Davydov and Kasha [2, 3], which usually takes place in crystalline semiconductors or molecular assemblies, where different sites of the crystalline lattice are excited simultaneously, providing an excited state of an ensemble of electrons and holes. On the other hand, the weak coupling regime is associated with the other important feature of exciton, *i.e.*, the excitonic (Förster) energy transfer. This was first mentioned by the inventor of exciton J. Frenkel in 1931, who also considered spreading of atomic excitation in a dielectric crystal [1]. In this case, the excitation can extend over two or more crystal subunits, but in a sequential, not coherent, mode, *i.e.*, it has both temporal and spatial dynamics. Thus, just

a dynamic nature makes a clear difference between the exciton and molecular or atomic excitation [4]. Therefore, a more precise definition of exciton can be found, for example, in *Collins English Dictionary* as “a *mobile* neutral entity in a crystalline solid consisting of an excited electron bound to the hole produced by its excitation” [5], or in *Encyclopedia Britannica* as “the combination of an electron and a positive hole (an empty electron state in a valence band), which *is free to move* through a nonmetallic crystal as a unit” [6].

The above aspects of the exciton properties also provide two viewpoints on the exciton size. The first one normally considers the exciton size as an average distance between electron and hole in the excited electron-hole pair, and the second viewpoint takes into account exciton delocalization, where the latter is determined by the center of mass distribution width, *i.e.*, where the wavefunction of the exciton is spatially located, or the space which electron-hole wave packet can explore coherently. The relationship between above two aspects of the exciton size can be seen on the following examples. First, J-aggregates of some organic dyes can consist of hundreds of molecules, but the exciton seizes a smaller amount, from few to several tens of molecules, respectively, which are excited coherently; this relatively large amount compared to size of Frenkel exciton constitutes the delocalization or coherence length of the exciton in J-aggregates, whereas the electron-hole separation in the Frenkel exciton is confined to one

molecule only. The other example concerns behavior of conjugated polymers. Whereas the mean electron-hole distance due to π - π^* excitations which are delocalized over the conjugated polymer chain and which have similar spatial overlap can be the same, the extent of exciton delocalization determined by the effective conjugation length may vary significantly for some polymers. Particularly, the exciton coherence length is different for the hot and cold excitons, because the hot excitons possessing a higher energy are more delocalized as compared to the relaxed cold excitons [7]. For example, delocalization of the hot exciton in poly(paraphenylenevinylene) (PPV) oligomers with the length of up to 14-mer occurs over the whole oligomer chain, whereas after vibrational relaxation of the hot one to the cold exciton excitation becomes distributed over about four repeat units [8].

In this work, the limitations of exciton size are discussed by analysis of the different excitation types (Fig. 1), where the exciton concept is still applicable. It is shown that the exciton size can be as small as few angstroms, but even smaller sizes can, probably, be justified. On the other hand, the exciton delocalization length can be as high as tens of micrometers due to self-interference with polariton modes in the optical cavity.

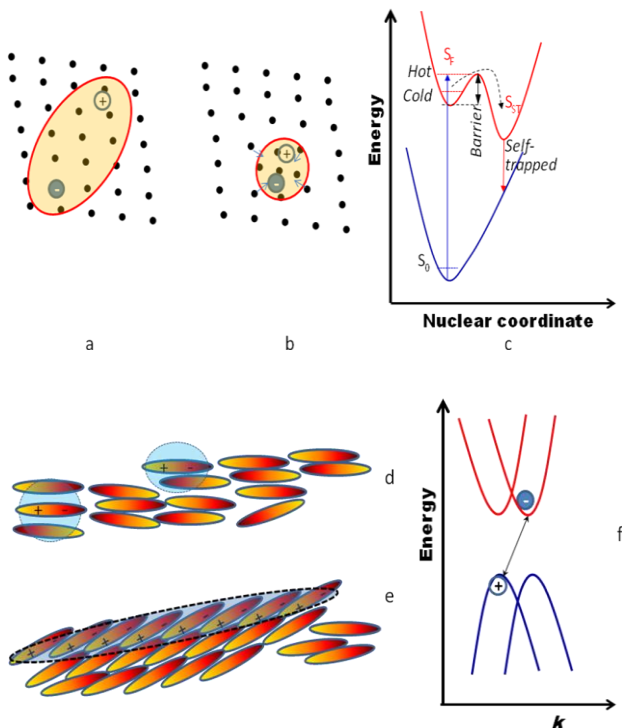


Fig. 1. Schematic presentation of excitons mentioned in the text: (a) Wannier–Mott exciton in a crystal lattice; (b) Self-trapped exciton (arrows indicate lattice distortion); (c) Energy scheme for excitation of free hot and cold excitons, and conversion to self-trapped exciton; (d) Frenkel excitons in a disordered ensemble of molecules; (e) Delocalized exciton in J-aggregate; (f) Energy scheme representing a Rashba exciton due to splitting in valence and conduction bands by spin-orbit coupling.

2. Low limit of the exciton size

We start from the analysis of low limit of exciton size. Here, Frenkel excitons in organic chromophores and the self-trapped exciton (STE) in organic and inorganic materials are relevant to consider, because these possess much smaller radius compared to the free Wannier–Mott exciton. A small size of Frenkel exciton is due to the low dielectric constant (relative permittivity) of an organic medium (usually $\epsilon \sim 1.5 \dots 4.0$), which causes high Coulombic attraction of electron and hole in the bound excited pair, whereas higher dielectric constants of semiconductor crystals (usually $\epsilon > 10$), provide much lower Coulombic attraction, lower binding energy and larger radius of Wannier–Mott exciton.

A one-electron atomic excitation gives rise to the smallest electron-hole distance called the Bohr radius [9],

$$a_B = \frac{\hbar}{m_e c \alpha}, \quad (1)$$

where \hbar is the reduced Planck constant, m_e – electron mass, c – light speed, and α – fine-structure constant. a_B is 0.053 nm, which corresponds to the Bohr radius in the hydrogen atom; however, even a smaller Bohr radius can be found in one-electron ions, such as He^+ and Li^{2+} (being $a_B/2$ and $a_B/3$, respectively), since the modified Bohr radius a_e depends on the reduced mass μ of the electron-nucleus pair, or the number of protons Z in the nucleus:

$$a_e = \frac{\epsilon m_0}{\mu Z} a_B, \quad (2)$$

$$\frac{1}{\mu} = \frac{1}{m_e^*} + \frac{1}{m_h^*}. \quad (3)$$

However, excitations in the above one-electron atoms or ions cannot be literally considered as exciton, since the exciton is a mobile excitation able for delocalization or migration (energy transfer), which is not the case here. Thus, a question may arise, what is the limited size/structure of a molecule beyond which the exciton concept does not work?

Beside crystals, the excitons in complex multi-electron molecules can be formally considered as a result of collective excitation too, due to electron-electron interactions and excitation delocalization over different fragments in a molecule. Scholes and Rumbles give an example of polyacene molecules, where lengthening of a benzene molecule by adding additional benzene units splits molecular energy levels and thus contributes to formation of the exciton band through combination of local single excitations; therefore, the authors state that in this case “the single-excitation configurations are mixed by exchange interactions so that each excited state – exciton state – is a linear combination of the single-excitation configurations” [10]. The same statement can be applied to linear conjugated chain, starting from ethylene molecule (Fig. 2). By adding new conjugated units, the HOMO and LUMO levels of the molecule split and transform to exciton bands. That is similar to situation

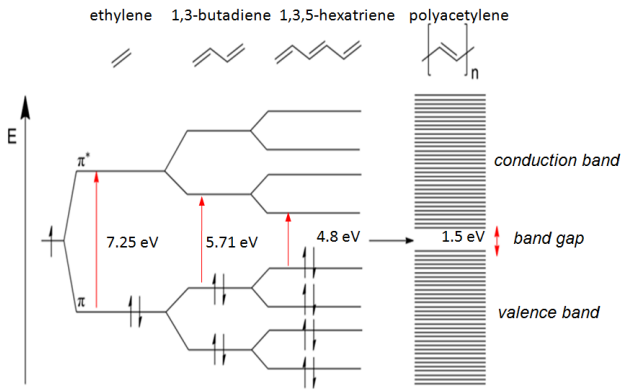


Fig. 2. Energy scheme of 1D conjugated chain showing an increasing splitting of the π and π^* molecular orbitals and formation of the exciton band with increasing amount of the conjugated bonds.

in a dimer, where two molecules are strongly coupled to each other, which leads to Davydov's splitting of the energy levels due to collective excitation of the both molecules [11]. Therefore, a 1,3-butadiene molecule (Fig. 2) probably can be considered as a smallest conjugated structure, where the exciton arises. The length of this molecule is 3.5 \AA [12], which should correspond to its exciton size. The other example includes a cluster of C_{60} with conjugated bonds. Due to the closed buckyball structure the exciton is confined to the buckyball dimension and has a size of 5 \AA (Table).

However, a smallest structure able to produce an exciton seems to consist of only two coupled atoms. Morrison *et al.* applied an exciton model to a linear chains of He atoms ($n = 2 \dots 30$), where the atomic excited states tend to be fully delocalized across the entire chain [13]. Simulation of the Frenkel–Davydov exciton started from the He_2 dimer (with each atom separated by the He_2 equilibrium distance of 1.581978 \AA), which can be taken as the smallest exciton size.

The other example of small excitons concerns donor-acceptor (D-A) systems where acceptor of energy is separated from donor of energy by only a few angstroms. In small molecules like rare-earth complexes the Förster energy transfer from the ligand to the metal ion can proceed over a distance of few angstroms. In the limit of the pure Dexter energy transfer which enables diffusion of triplet excitons, energy flow proceeds between D and A that are closely contact by transfer of the excited electron of D to the excited level of A, followed by a second (or concerted) exchange of electron that occurs from the A ground state to the D ground state, with the electron transfer rate k described by Eq. (4):

$$k = A \exp(-\beta[r - r_0]), \quad (4)$$

where β is a medium-dependent property describing the decay of the inverse tunneling distance of an electron between donor and acceptor, which can be taken as the inverse length of triplet exciton. You *et al.* found that for triplet-triplet coupling between a pair of face-to-face ethylene molecules, the exponential attenuation factor is

2.59 \AA^{-1} , which is about twice as large as typical values for electron transfer [14]. However, even a larger computed attenuation factor (respectively smaller exciton energy transfer distance) up to 5.14 \AA^{-1} was reported by Curutchet and Voityuk for the Dexter transport [15].

3. Exciton size in low-dimensional media

Spatial dimensionality D of the system largely influences localization-delocalization dynamics of exciton. First, the excitation process differs greatly in 1D and 3D systems. In bulk 3D semiconductors, the exciton has a binding energy of the excited electron-hole pair, which is compared to or smaller than kT (T – room temperature), and a weak Coulomb interaction of the order of few meV, respectively. Therefore, such excitons are mostly dissociated after the excitation. Exciton binding energies increase in low-dimensional systems and are one to two orders of magnitude larger in typical quasi-1D semiconductors such as conjugated chains, leading to that the 1D excitons are bound tightly, possess small radius and undergo ease recombination. These properties follow from the simple hydrogenic Schrodinger equation in the fractional-dimensional space [16], which provides the exciton radius r_e and the binding energy E_b of the 1s exciton as a function of D :

$$r_e = ((D-1)/2)^2 a_B, \quad (5)$$

$$E_b = (2/(D-1))^2 E_e, \quad (6)$$

where E_e is the effective Rydberg constant. It follows from Eqs (5) and (6) that in an ideal 1D system the exciton should be squeezed to a negligibly small radius, because of infinitely large Coulomb energy. As a result, this leads to remarkable changes of the exciton size in 2D systems such as transition metal dichalcogenides (TMDCs). For example, the Wannier–Mott excitons in bulk MoS_2 , which originate from the vertical band-to-band transitions, have the size of 2.35 (exciton A) and 1.74 nm (exciton B), whereas they shrink to 1.0 and 0.8 nm, respectively, in monolayer of MoS_2 (Table). Interesting features of excitons are that they can originate due to splitting in valence and conduction bands by spin-orbit coupling, the so-called Rashba effect [17, 18]. For this exciton (exciton C), which originates from the indirect band-to-band transitions due to the Rashba effect [19, 20] (Fig. 1f), the changes in size are even more dramatic, being 5.53 and 1.8 nm for the 3D and 2D excitons, respectively (Table).

The other property of excitons in low-dimensional systems is self-trapping effect that leads to significant squeezing of the initial delocalization of the excitation to a size of the order of the lattice constant. The exciton self-trapping mostly occurs due to the strong exciton-lattice coupling, but it takes place only if the chain is deformable, which results in a chain distortion that produces a new polaronic state below the exciton band bottom [21]. A strong electron-phonon coupling is a remarkable feature of 1D electronic systems, which leads to the dynamic torsional disorder along the 1D chain and the exciton self-trapping [4].

Table. Exciton size in excitations of the different type.	
Structure/Excitation type	Exciton size/Reference
Hydrogen/single-electron excitation	0.053 nm (Bohr radius)*
He ₂ dimer/Frenkel exciton	0.16 nm [13]
1,3-butadiene/Frenkel exciton	0.35 nm (see text)
D-A systems/Dexter energy transfer	<0.5 nm (see text)
C ₆₀ /Frenkel exciton	0.5 nm [30]
Semiconductor crystals/self-trapped exciton	of the order of the lattice constant (<i>e.g.</i> , 0.56 nm for GaAs)
One-dimensional molecules with a size longer than ~4 nm/ Frenkel exciton	0.7 nm [30]
2D TMDC MoS ₂ /Low-dimensional exciton	1.0 nm (direct exciton A) 0.8 nm (direct exciton B) 1.8 nm (indirect/ Rashba exciton C) [39]
3D MoS ₂ /Wannier–Mott exciton	2.35 nm (direct exciton A) 1.74 nm (direct exciton B) 5.53 nm (indirect/Rashba exciton C) [39]
Hybrid perovskite CH ₃ NH ₃ PbI ₃ /Rashba exciton	2.5 nm [40]
PPV polymer/delocalized Frenkel exciton	~ 2.5...3.5 nm (see text)
DNTT/delocalized Frenkel exciton	~ 9 nm (14-15 molecules) [32]
ZnS/Wannier–Mott exciton	1.5 nm
ZnO/Wannier–Mott exciton	2 nm [41]
CdS/Wannier–Mott exciton	3 nm [41]
Carbon nanotubes/Wannier–Mott exciton	2 nm [27] 3.5...13 nm [42] 13 nm [28]
Linear aggregate of C ₆₀ /Wannier–Mott exciton	~ 5...7 nm [45]
Si/ Wannier–Mott exciton	9 nm [43]
11-armchair graphene nano-ribbon/Wannier–Mott exciton	10 nm [44]
GaAs/Wannier–Mott exciton	12 nm [41]
PbS/Wannier–Mott exciton	18 nm [41]
InAs/Wannier–Mott exciton	38 nm [41]
Optical microcavity/Exciton–polariton	20 μm [38]

*Hydrogen Bohr radius is given for the comparison; it is not associated with the exciton.

Self-trapping depends strongly on dimensionality of the exciton delocalization pathway, and in 1D systems the excitons should be always self-trapped, because the self-trapping minimum lies lower than that of the free exciton (Fig. 1c), and there is a lack of any energy barrier between free and self-trapped excitonic states, as it was predicted in the theory developed by Rashba and Toyozawa [22, 23]. In addition, because a strong electron-phonon coupling exists in 1D electronic systems, this leads to the dynamic torsional disorder along the 1D chain. The electron-phonon coupling is a function of length of the 1D system, and it increases in shorter molecules with smaller amount of π -conjugated bonds; particularly, it increases linearly for the linear aromatic acenes as a function of the inverse number of carbon atoms in the molecule [24]. For example, within tens of fs

from photoexcitation a singlet Frenkel exciton in P3HT single molecules becomes delocalized over ~15 monomer units, which can be considered as a kind of charge-transfer (CT) exciton with quasi-free electrons and holes capable for ultrafast coherent charge transfer of the primary photoexcited carriers [25]. Then, localization of the above charge carriers to the bound exciton or exciton self-trapping to less than 10 monomers units takes place within ~ 100 fs due to the local structural chain distortion or twisting.

However, some low-dimensional systems, particularly, carbon nanotubes and graphene nano-ribbons, indicate unusual behavior of exciton with rather large exciton size of the order of 10 nm (Table). In carbon nanotubes, although the exciton Bohr radius along the tube axis was assessed to be ~ 1 nm [26], the measured

values revealed that the exciton size varies from 2 [27] to 13 nm [28]. This unexpectedly large exciton size in carbon nanotubes is due to the fact that the exciton in this 1D system is sensitive to dielectric constant of the environment that renders a screening effect on exciton transition and binding energies, thus reducing the electron-hole interactions and enlarging the exciton size [28].

4. Upper limit of the exciton size

The Wannier–Mott exciton has a larger radius (usually above 1 nm) as compared to the Frenkel exciton, since the electron-hole pair is bound by a weaker electrostatic force due to usually high dielectric constant of the medium. For example, in the InAs crystal, the Wannier–Mott exciton size can be as large as 38 nm (Table). However, a large exciton size can be found in the Frenkel exciton too, due to delocalization of excitation over two or more subunits associated with the delocalization across heterojunction, over conjugated chain or molecular assembly, where the different subunits are excited coherently. Exciton delocalization across a heterojunction with electron located at the acceptor and hole at the donor counterpart, *i.e.*, formation of the CT exciton, depends on the donor-acceptor architecture (face-on or edge-on orientation of the moieties) and exciton energy (hot or cold), leading to exciton size variation from 0.9 to 2.4 nm for the system of PCBM fullerene acceptor and dual-band donor polymer composed of thiophene, benzothiadiazole, and benzotriazole subunits [29]. Mewes *et al.* found that the Frenkel exciton has a saturation length of 0.7 nm in 1D chains longer than 4 nm [30], however, Tretiak *et al.* calculated that in PPV polymer due to delocalization, the coherence length of the delocalized exciton constitutes 5-7 monomer units ($\sim 2.5\text{--}3.5$ nm) [31]. Tanaka *et al.* reported an exciton coherence length in dinaphtho[2,3-*b*:2,3-*f*]thieno[3,2-*b*]thiophene (DNTT) crystals to be 14-15 molecules (*i.e.*, about ~ 9 nm), whereas this value increases up to 40 molecules upon alkyl-chain substitution in C₁₀-DNTT crystals [32]. The exciton coherence length in J-aggregates of pseudoisocyanine can be as much as over 100 molecules [33, 34], that is, about ~ 100 nm.

Other options that assist in formation of ultralong exciton delocalization include surface plasmon-polaritons and optical cavities. Quenzel *et al.* demonstrated that the exciton coherence length of squaraine aggregates can be increased from 10 to 24 molecular units at room temperature in the presence of plasmon mode due to the radiative coupling of localized, energetically nearly resonant excitons on the molecular units and delocalized surface plasmon-polariton modes at a planar molecule – gold interface [35]. Optical cavity can produce photons as a result of exciton decay, which can oscillate long enough including the processes of reabsorption, reemission, and so on. The entangled exciton-photon eigenstates then lead to formation of cavity polaritons, wave functions of which extend over large distances well exceeding the molecular length. The strong coupling regime between the exciton and photon provides both

a large delocalization length of the exciton and ultralong energy transport well beyond the Förster limit due to the entangled and delocalized nature of the polaritonic states. In this case, the energy transfer efficiency can reach up to 37% for donor-acceptor distances ≥ 100 nm [36]. Exciton-polariton modes can be generated due to coupling of a Bloch surface wave photon with molecular excitons mediated by optical microcavities containing a disordered excitonic material, where the delocalized exciton-polariton possesses a group velocity as high as $3 \cdot 10^7$ m·s⁻¹ and the lifetime close to 500 fs, leading to propagation distances of over 100 μ m from the excitation source, whereas the exciton-polariton coherence length, *i.e.*, exciton delocalization, is as high as 20 μ m due to self-interference of the polariton mode [37, 38].

5. Conclusions

Being based on the above analysis, it can be concluded that the exciton size is largely dependent on material and excitation conditions, and it can span as much as five orders of magnitude. The low limit, which is relevant to the Frenkel exciton in two-atomic molecule, small conjugated molecules like 1,3-butadiene, or donor-acceptor rare-earth complexes with Dexter energy transfer, is usually less than 0.5 nm and can be as small as 0.16 nm. This value, however, is larger than the hydrogen Bohr radius by at least three times, which makes a clear difference between the exciton and a local molecular/atomic excitation. On the other hand, the upper limit of exciton size can be considered as an exciton delocalization length in multichromophoric systems or ordered assemblies, where multiple subunits can be excited coherently. In this case, the exciton size can be extended to over 100 nm. However, optical cavities render even more significant impact on exciton delocalization, providing the lengthening of the exciton size through self-interference with the polariton mode, which yields the exciton delocalization length to be as high as tens of micrometers. The above significant scales of changes that the exciton size can experience provide exciting opportunities for relevant applications of exciton-related phenomena in photonics and optoelectronics.

References

1. Frenkel J. On the transformation of light into heat in solids. I. *Phys. Rev.* 1931. **37**. P. 17–44. <https://doi.org/10.1103/PhysRev.37.1276>.
2. Davydov A.S. The theory of molecular excitons. *Sov. Phys. Usp.* 1964. **7**. 145–186. <http://iopscience.iop.org/0038-5670/7/2/R01>.
3. Kasha M., Rawls H.R., El-Bayoumi M.A. The exciton model in molecular spectroscopy. *Pure Appl. Chem.* 1965. **11**. P. 371–392. <https://doi.org/10.1351/pac196511030371/html>.
4. Dimitriev O.P. Dynamics of excitons in conjugated molecules and organic semiconductor systems. *Chem. Rev.* 2022. **122**. P. 8487–8593. <https://doi.org/10.1021/acs.chemrev.1c00648>.

5. <https://www.collinsdictionary.com/dictionary/english/exciton>.
6. Britannica, The Editors of Encyclopaedia. "exciton". *Encyclopedia Britannica*, 20 Jul. 1998, <https://www.britannica.com/science/exciton>. Accessed 8 August 2022.
7. Kafle T.R., Kattel B., Wang T., Chan W.-L. The relationship between the coherent size, binding energy and dissociation dynamics of charge transfer excitons at organic interfaces. *J. Phys.: Condens. Matter*. 2018. **30**, No 45. P. 454001. <https://doi.org/10.1088/1361-648X/aae50b>.
8. Tretiak S., Saxena A., Martin R.L., Bishop A.R. Conformational dynamics of photoexcited conjugated molecules. *Phys. Rev. Lett.* 2002. **89**. P. 097402. <https://doi.org/10.1103/PhysRevLett.89.097402>.
9. Griffiths D.J. *Introduction to Quantum Mechanics*. Prentice-Hall. 1995. P. 137.
10. Scholes G.D., Rumbles G. Excitons in nanoscale systems. *Nat. Mater.* 2006. **5**. P. 683–696. <https://doi.org/10.1038/nmat1710>.
11. Zhong C., Bialas D., Collison C.J., Spano F.C. Davydov splitting in squaraine dimers. *J. Phys. Chem. C*. 2019. **123**. P. 18734–18745. <https://doi.org/10.1021/acs.jpcc.9b05297>.
12. Craig N.C., Groner P., McKean D.C. Equilibrium structures for butadiene and ethylene: compelling evidence for π -electron delocalization in butadiene. *J. Phys. Chem. A*. 2006. **110**. P. 7461–7469. <https://doi.org/10.1021/jp060695b>.
13. Morrison A.F., You Z.Q., Herbert J.M. *Ab initio* implementation of the Frenkel–Davydov exciton model: A naturally parallelizable approach to computing collective excitations in crystals and aggregates. *J. Chem. Theory Comput.* 2014. **10**. P. 5366–5376. <https://doi.org/10.1021/ct500765m>.
14. You Z.Q., Hsu C.P., Fleming G.R. Triplet-triplet energy-transfer coupling: Theory and calculation. *J. Chem. Phys.* 2006. **124**. P. 044506. <https://doi.org/10.1063/1.2155433>.
15. Curutchet C., Voityuk A.A. Distance dependence of triplet energy transfer in water and organic solvents: A qm/md study. *J. Phys. Chem. C*. 2012. **116**. P. 22179–22185. <https://doi.org/10.1021/jp306280y>.
16. He X.F. Excitons in anisotropic solids: the model of fractional-dimensional space. *Phys. Rev. B*. 1991. **43**. P. 2063–2068. <https://doi.org/10.1103/PhysRevB.43.2063>.
17. Jantayod A. Unconventional Rashba spin-orbit coupling on the charge conductance and spin polarization of a ferromagnetic/insulator/ferro-magnetic Rashba metal junction. *Micromachines*. 2022. **13**. P. 1340. <https://doi.org/10.3390/mi13081340>.
18. Lafalce E., Amerling E., Yu Z.G. *et al.* Rashba splitting in organic–inorganic lead–halide perovskites revealed through two-photon absorption spectroscopy. *Nat. Commun.* 2022. **13**. P. 483. <https://doi.org/10.1038/s41467-022-28127-9>.
19. Rashba E.I. Symmetry of energy bands in crystals of wurtzite type: I. Symmetry of bands disregarding spin-orbit interaction. *Sov. Phys. Solid State*. 1959. **1**. P. 368–380.
20. Rashba E.I. and Sheka V.I. Symmetry of energy bands in crystals of wurtzite type II. Symmetry of bands with spin-orbit interaction included. *New. J. Phys.* 2015. **17**. P. 050202. Originally published in *Fiz. Tverd. Tela: Collected Papers*. 1959. **2**. P. 62–76. http://iopscience.iop.org/1367-2630/17/5/050202/media/njp050202_suppdata.pdf.
21. Katrich G.S., Kemnitz K., Malyukin Y.V., Ratner A.M. Distinctive features of exciton self-trapping in quasi-one-dimensional molecular chains (J-Aggregates). *J. Lumin.* 2000. **90**. P. 55–71. [https://doi.org/10.1016/S0022-2313\(99\)00609-2](https://doi.org/10.1016/S0022-2313(99)00609-2).
22. Rashba E.I. Theory of strong interactions of electron excitations with lattice vibrations in molecular crystals. 2. *Optika i Spektroskopiya*. 1957. **2**. P. 88–98.
23. Toyozawa Y. Self-trapping of an electron by the acoustical mode of lattice vibration. I. *Prog. Theor. Phys.* 1961. **26**. P. 29–44. <https://doi.org/10.1143/PTP.26.29>.
24. Brédas J.-L., Beljonne D., Coropceanu V., Cornil J. Charge-transfer and energy-transfer processes in π -conjugated oligomers and polymers: a molecular picture. *Chem. Rev.* 2004. **104**. P. 4971–5004. <https://doi.org/10.1021/cr040084k>.
25. Banerji N., Cowan S., Vauthey E., Heeger A.J. Ultrafast relaxation of the poly(3-hexylthiophene) emission spectrum. *J. Phys. Chem. C. Nanomater. Interfaces*. 2011. **115**. P. 9726–9739. <https://doi.org/10.1021/jp1119348>.
26. Miyauchi Y., Hirori H., Matsuda K., Kanemitsu Y. Radiative lifetimes and coherence lengths of one-dimensional excitons in single-walled carbon nanotubes. *Phys. Rev. B*. 2009. **80**. P. 081410. <https://doi.org/10.1103/PhysRevB.80.081410>.
27. Lüer L., Hoseinkhani S., Polli D. *et al.* Size and mobility of excitons in (6, 5) carbon nanotubes. *Nature Phys.* 2009. **5**. P. 54–58. <https://doi.org/10.1038/nphys1149>.
28. Mann C., Hertel T. 13 nm exciton size in (6, 5) single-wall carbon nanotubes. *J. Phys. Chem. Lett.* 2016. **7**. P. 2276–2280. <https://doi.org/10.1021/acs.jpcclett.6b00797>.
29. Varella M.T.D.N., Stojanovic L., Vuong V.Q. *et al.* How the size and density of charge-transfer excitons depend on heterojunction’s architecture. *J. Phys. Chem. C*. 2021. **125**. P. 5458–5474. <https://doi.org/10.1021/acs.jpcc.0c10762>.
30. Mewes S.A., Plasser F., Dreuw A. Universal exciton size in organic polymers is determined by nonlocal orbital exchange in time-dependent density functional theory. *J. Phys. Chem. Lett.* 2017. **8**. P. 1205–1210. <https://doi.org/10.1021/acs.jpcclett.7b00157>.

31. Tretiak S., Igumenshchev K., Chernyak V. Exciton sizes of conducting polymers predicted by time-dependent density functional theory. *Phys. Rev. B*. 2005. **71**. P. 033201. <https://doi.org/10.1103/PhysRevB.71.033201>.
32. Tanaka S., Miyata K., Sugimoto T. *et al.* Enhancement of the exciton coherence size in organic semiconductor by alkyl chain substitution. *J. Phys. Chem. C*. 2016. **120**. P. 7941–7948. <https://doi.org/10.1021/acs.jpcc.5b12686>.
33. Kobayashi S., Sasaki F. Ultrafast spectroscopy of PICBr J aggregates: the dynamics of large coherence length exciton. *J. Lumin.* 1994. **58**. P. 113–116. [https://doi.org/10.1016/0022-2313\(94\)90373-5](https://doi.org/10.1016/0022-2313(94)90373-5).
34. Fidler H., Terpstra J., Wiersma D.A. Dynamics of Frenkel excitons in disordered molecular aggregates. *J. Chem. Phys.* 1991. **94**. P. 6895–6907. <https://doi.org/10.1063/1.460220>.
35. Quenzel T., Timmer D., Gittinger M. *et al.* Plasmon-enhanced exciton delocalization in squaraine-type molecular aggregates. *ACS Nano*. 2022. **16**. P. 4693–4704. <https://doi.org/10.1021/acsnano.1c11398>.
36. Zhong X., Chervy T., Zhang L. *et al.* Energy transfer between spatially separated entangled molecules. *Angew. Chem. Int. Ed.* 2017. **56**. P. 9034–9038. <https://doi.org/10.1002/anie.201703539>.
37. Rozenman G.G., Akulov K., Golombek A., Schwartz T. Long-range transport of organic exciton-polaritons revealed by ultrafast microscopy. *ACS Photonics*. 2018. **5**. P. 105–110. <https://doi.org/10.1021/acsp Photonics.7b01332>.
38. Hou S., Khatoniari M., Ding K. *et al.* Ultralong-range energy transport in a disordered organic semiconductor at room temperature *via* coherent exciton-polariton propagation. *Adv. Mater.* 2020. **32**. P. 2002127. <https://doi.org/10.1002/adma.202002127>.
39. Jia G.Y., Liu Y., Gong J.Y. *et al.* Excitonic quantum confinement modified optical conductivity of monolayer and few-layered MoS₂. *J. Mater. Chem. C*. 2016. **4**. P. 8822–8828. <https://doi.org/10.1039/C6TC02502A>.
40. Ma J., Wang L.W. Nanoscale charge localization induced by random orientations of organic molecules in hybrid perovskite CH₃NH₃PbI₃. *Nano Lett.* 2015. **15**. P. 248–253. <https://doi.org/10.1021/nl503494y>.
41. Singh B.P. Optoelectronic and nonlinear optical processes in low dimensional semiconductors. *Bull. Mater. Sci.* 2006. **29**. P. 559–565. <https://doi.org/10.1007/s12034-006-0004-3>.
42. Kilina S., Tretiak S., Doorn S.K. *et al.* Cross-polarized excitons in carbon nanotubes. *Proc. Natl. Acad. Sci. USA*. 2008. **105**, No 19. P. 6797–6802. <https://doi.org/10.1073/pnas.0711646105>.
43. Hiramoto M., Kubo M., Shinmura Y. *et al.* Bandgap science for organic solar cells. *Electronics*. 2014. **3**. P. 351. <https://doi.org/10.3390/electronics3020351>.
44. Wang M., Li C.M. Excitonic properties of graphene-based materials. *Nanoscale*. 2012. **4**. P. 1044–1050. <https://doi.org/10.1039/C1NR10885A>.
45. Morkath J.H. Delocalized exciton formation in C60 linear molecular aggregates. *Phys. Chem. Chem. Phys.* 2021. **23**. P. 21901–21912. <https://doi.org/10.1039/D1CP02430B>.

Author and CV



Oleg Dimitriev, Senior research fellow at the V. Lashkaryov Institute of Semiconductor Physics, NAS of Ukraine. Also, he serves as Assistant Professor at the National Technical University of Ukraine “Igor Sikorsky Kyiv Polytechnic Institute”. His major research interests are focused on photophysics of organic polymers and dyes but also include other issues, namely: materials science of organic and hybrid heterostructures, energy conversion, and ecological thinking. He is a recipient of international awards from Swedish Institute, Fulbright Visiting Scholar Program, German Academic Exchange Service (DAAD), and Japan Society for the Promotion of Science (JSPS). He is the author of popular science books *Sensible Universe* and *What Does Your Clock Show?*

Розмір екситона: де межі?

О.П. Дімітрієв

Анотація. Поняття екситону передбачає колективний збуджений стан, здатний рухатися як частинка. Його розмір визначається радіусом збудженої електрон-діркової пари, і, хоча він може змінюватися на два порядки величини, він завжди просторово обмежений, тоді як його довжина делокалізації завдяки просторовій динаміці хвильової функції екситону може забезпечити навіть більший масштаб змін. У цій роботі обмеження розмірів екситонів обговорюються шляхом аналізу, де концепція екситонів все ще має місце. Показано, що розмір екситону може бути всього лише кілька ангстрем, але навіть менші розміри, ймовірно, можуть бути виправданими. У той же час зв'язок екситону з поляритонною модою може збільшити довжину когерентності екситонного поляритону до значень 20 мкм, таким чином розширюючи масштаб можливих розмірів екситонів до п'яти порядків.

Ключові слова: екситон Ваньє–Мотта, екситон Френкеля, делокалізація, автозахоплення, низькорозмірне середовище, ефект Рашби.